Towards a spectral library of Roman to Early Christian Cypriot floor mosaics

V. Lysandrou [a,*], D. Cerra [b], A. Agapiou [a], E. Charalambous [c], D.G. Hadjimitsis [a]

[a] Department of Civil Engineering and Geomatics, Faculty of Engineering and Technology, Cyprus University of Technology, 2-6, Saripolou str., 3603 Limassol, Cyprus
[b] German Aerospace Center (DLR), Earth Observation Center (EOC), 82234 Weßling, Germany
[c] Department of Antiquities of Cyprus, 1 Museum Avenue, 22024, Nicosia 1516, Cyprus

ARTICLE INFO

ABSTRACT

Floor mosaics are of great interest for archaeologists and art historians. While in the last decade other scientific sectors supported their study mainly from a technical point of view, through traditional archaeometric analysis, this paper suggests an innovative methodological approach and presents some preliminary results aiming to a non-destructive investigation based on the spectroradiometric analysis of stones used for manufacturing the ancient floor mosaics of Cyprus. This method evaluates the results of spectroradiometric analysis in relation to reliable destructive analysis completed in the past on the hereunder examined samples. In addition, the results of the proposed approach foresee to contribute to the expansion of the existing Cypriot database of floor mosaics, improving their characterization by collecting their spectral signatures in the range of 350–2500 nm. The proposed methodology has been applied to a number of stone samples directly linked to pavement floor mosaic tesserae from Cyprus. The results have shown that spectroradiometers may be used in order to identify mineralogical compositions of the stones with an accuracy of nearly 90%. To the best of our knowledge, this is the first time that a comprehensive spectral library related to Cyprus floor mosaics is derived.

1. Introduction

A series of complex and unique geological processes have made Cyprus a geological model for the earth scientists worldwide, and has been the primary factor in the creation of the island's natural environment (Dep. Geol. Surv., 2002) (Fig. 1). The singularity of Cypriot geology has played an important role in the course of history and helped significantly the cultural and socio-economic growth and development of the island.

Moreover, the geological variety of Cyprus contributed significantly to the development of the mosaic art on the island. The vast chromatic spectrum of the rocks along with their mechanical properties offered the opportunity to this form of art to flourish and manifest through exceptional examples, allowing the mosaic artisans of ancient times to create magnificent masterpieces and to experiment through their work. The Mamonian Complex provided the main material source for these artefacts (Charalambous et al., 2009a; Charalambous, 2011). The complex itself, as well as the Fasoula formation, was until recently the main source of primary material for the mosaic artisans, even of recent times (Charalambous et al., 2009a).

Ancient floor mosaics represent one of the greatest artistic expressions of the spirit of Hellenistic and Roman art in Cyprus, with the most exceptional examples dating to the late Roman, early Christian and Byzantine periods (Fig. 2) (Michaelides, 1987; Charalambous, 2012). These mosaics represent one of the most important sectors of art and archaeology for Cyprus for an extensive period of the ancient history of the island, and provide significant information regarding the trends of the corresponding periods both in terms of stylistic preferences and manufacturing technologies employed, including techniques and materials used. Therefore, the study of the floor mosaics of Cyprus, especially of the Roman, late Roman and early Byzantine periods (2nd–7th century CE), is considered very important for different scientific sectors principally including archaeology, art history, archaeometry and mosaic conservation (Charalambous et al., 2009a; Charalambous et al., 2009b; Hadjicosti and Charalambous, 2011; Charalambous, 2012).

A comprehensive and detailed study of the manufacturing technology of floor mosaics in Cyprus was recently compiled by Charalambous (2012). In his work, among the various aspects of the floor mosaics taken into account, a special effort was given in identifying the geological provenance of the stone tesserae of mosaic pavements all over the island. A number of natural rocks and stone mosaic tesserae were analyzed in terms of microscopic observation, colorimetric analysis and diffractometry to determine their mineralogical composition. The achieved result evidenced the provenance of stone mosaic tesserae and their correlation to specific geological formations of the island. In

* Corresponding author.
  E-mail addresses: vasiliki.lysandrou@cut.ac.cy (V. Lysandrou), daniele.cerra@dlr.de (D. Cerra), athos.agapiou@cut.ac.cy (A. Agapiou), eharalamb@yahoo.gr (E. Charalambous), d.hadjimitsis@cut.ac.cy (D.G. Hadjimitsis).
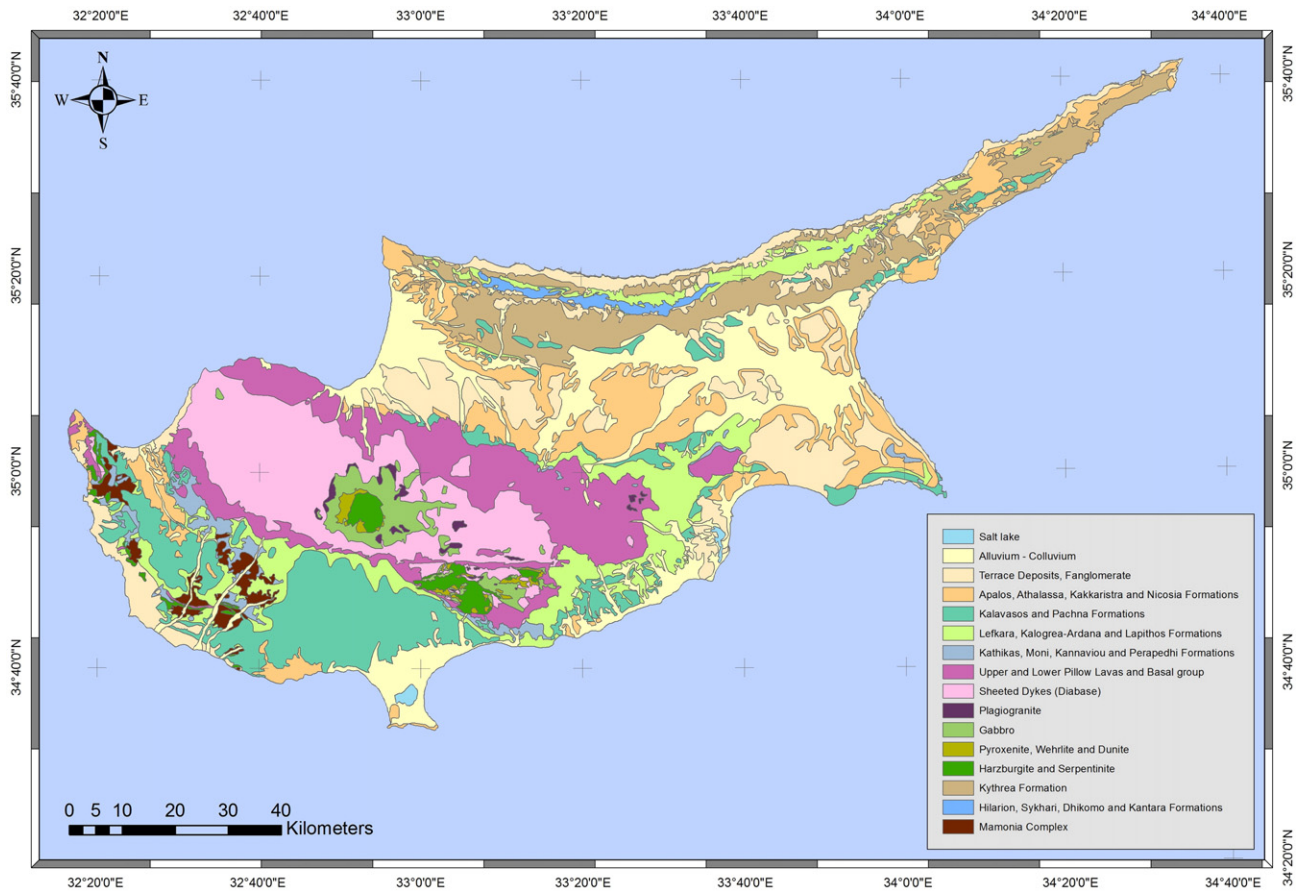
Fig. 1. Geological map of Cyprus.

Fig. 2. Nea Paphos: floor mosaic pavement from the 'Villa of Theseus' 3rd–4th century CE (photo taken by Dr. E. Charalambous).

addition, it contained a detailed list reproducing all floor mosaics on the island where the examined tesserae had been found.

As results from the literature (Bonnerot et al., 2015; Piovesan et al., 2014; Calia et al., 2013), the characterization employed for the mosaics manufacturing is usually performed based on destructive laboratory techniques and their study needs the involvement of experts specialized in this topic. Visual inspection of the samples remains a critical parameter for any kind of preservation and action needed in order to match each mosaic with the correct bedrock. Within the framework of visual inspection, this study aims to expand the available collected knowledge by building a spectral signature library for the case study of Cyprus, with the spectrometric analysis carried out in the range 350–2500 nm. The spectra contained in the library have been acquired using the HSV HR-1024 spectrometer, which covers the visible, the near infrared, and the short wave infrared portions of the spectrum. It must be specified that the purpose of such analysis is not replacing the already established techniques used for the study of the floor mosaics, but rather assisting experts to evaluate the likelihood that a previously unseen mosaic floor is composed by an already "known" material.

Ground spectroradiometers are non-invasive and non-destructive instruments and therefore can be easily integrated in the study of floor mosaics, and have beenused in the past for supporting archaeological research, e.g. for the identification of buried archaeological remains (i.e. crop marks) or to study geological formations for remote sensing applications (Agapiou and Hadjimitsis, 2011; Alexakis et al., 2012).

The paper is structured as follows: in Section 2 the overall methodology of the study is presented along with the equipment used. The spectral signatures of all samples are described in Section 3, while Section 4 focuses on the application ofstate of the art spectral analysis techniquesto retrieve reliable and robust categorization results for the available samples. The paper concludes with Section 5 highlighting some of the potential use of this approach within archaeological research of floor mosaics, as well as the overall novelty of the work and possible future expansions.

2. Methodology

The flowchart in Fig. 3 evidences the methodological approach of the spectroradiometric analysis.
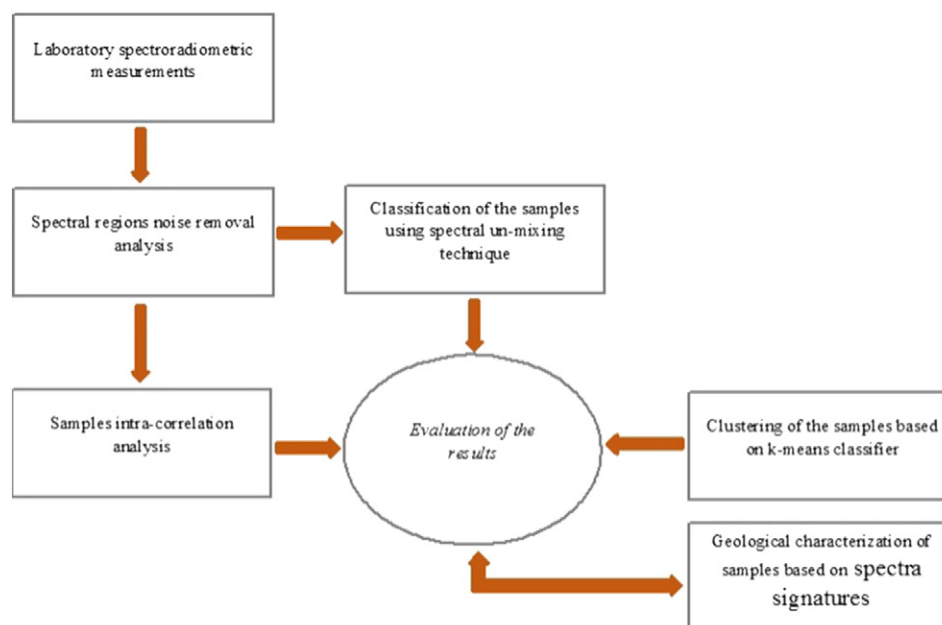
Laboratory spectroradiometric measurements were taken for 35 samples of bedrock which have been employed in ancient Cypriote floor mosaics. The spectra have been acquired with the HSV HR-1024 spectroradiometer, which features a spectral range from 350 nm to 2500 nm and 1024 spectrally narrow bands. The time needed for the acquisition of the spectral signature is in the interval of 1–10 ms and the data are stored in ASCII format. The Field of View (FOV) was set to 4°.

A detailed catalogue of the samples is provided in Fig. 4. For each sample a detailed mineralogical analysis using mainly X-ray diffractometry has been carried out by Charalambous (2012), indicating the percentage of the various minerals composing every single sample. For instance, the bedrock for sample 1 (Ash limestone) is composed by 98% of calcite and 2% of quartz. The mineralogical composition of all samples examined in the present study is given in Table 1 (see Section 3). For each sample five spectral measurements were recorded, and for each measurement the instrument was set to calculate the mean value of three simultaneous spectral profiles. The measurements were taken in the dark room of the Cyprus University of Technology, and a reference spectralon panel was used for calibrating the incoming radiance. The spectroradiometer was placed in a close proximity to the samples (approximately at a distance of 10 cm in a nadir view).

Subsequently, the measurements were analyzed in order to remove noisy spectral regions, and the intra-correlation between the samples was calculated. Finally, spectral unmixing techniques were applied in order to classify the samples into homogenous groups based on their mineralogical composition (Fig. 5).

The overall methodology applied in this study is composed by six main steps, as follows: (1) Clustering of the samples based on k-means classifier; (2) Laboratory spectroradiometric measurements; (3) Analysis and removal of noisy spectral bands; (4) Samples intra-correlation analysis (identification of the most relevant spectral bands based on mutual information); (5) Classification of the samples using spectral unmixing techniques and (6) Evaluation of the results.

3. Spectral signatures

Fig. 6 presents the spectroradiometric measurements for several samples of Fig. 4, for the range 350–2500 nm. Some spectral regions exhibiting a low Signal-to-Noise Ratio (SNR) (e.g. 350–400 nm) were removed from the graph. Several samples have similar spectral

Fig. 3. Flowchart evidencing the main steps of spectroradiometric analysis.

responses with relative low reflectance values (less than 35% for each band in the spectral range under examination). Therefore, a critical aspect of this study was to identify spectral regions that are more informative for the discrimination of the samples, and to cluster the different materials by finding natural groupings among them, verifying their correspondence to the different mineralogical compositions.

Table 1 summarizes the percentage of mineralogical composition of each sample examined in this study. Several samples are mainly composed by calcite with some exceptions such as sample 16 (75% Feldspar) or sample 19 (71% Feldspar) etc. The last three columns report the results of grouping materials with homogenous mineralogical composition through unsupervised clustering using the k-means classifier using as

Sample 1	Sample 2	Sample 3
Ash limestone	*White limestone*	*Green limestone*
Sample 4	Sample 5	Sample 6
Chestnut/brown limestone	*Grey limestone*	*Limestone*
Sample 7	Sample 8	Sample 9
Limestone	*Grey limestone*	*Grey-green limestone*
Sample 10	Sample 11	Sample 12
Siliceous limestone	*Red limestone*	*Limestone*
Sample 13	Sample 14	Sample 15
Limestone	*Reddish limestone*	*Reddish limestone*
Sample 16	Sample 17	Sample 18

Fig. 4. The table reproduces the photographic documentation of the samples examined in this study.

Brown/green limestone	***Amber limestone***	***Reddish limestone***
Sample 19	Sample 20	Sample 21
Red limestone	***Limestone***	***Limestone***
Sample 22	Sample 23	Sample 24
Red limestone	***Limestone***	***Limestone***
Sample 25	Sample 26	Sample 27
Limestone	***Brown-red limestone***	***Limestone***
Sample 28	Sample 29	Sample 30
Limestone	***Pinkish limestone***	***Light grey limestone***
Sample 31	Sample 32	Sample 33
Ash-brown limestone	***Grey-green limestone***	***Limestone***
Sample 34	Sample 35	
Siliceous limestone	***Brown-red limestone***	

Table 1
Mineralogical composition of the samples and the results from k-means unsupervised classification.

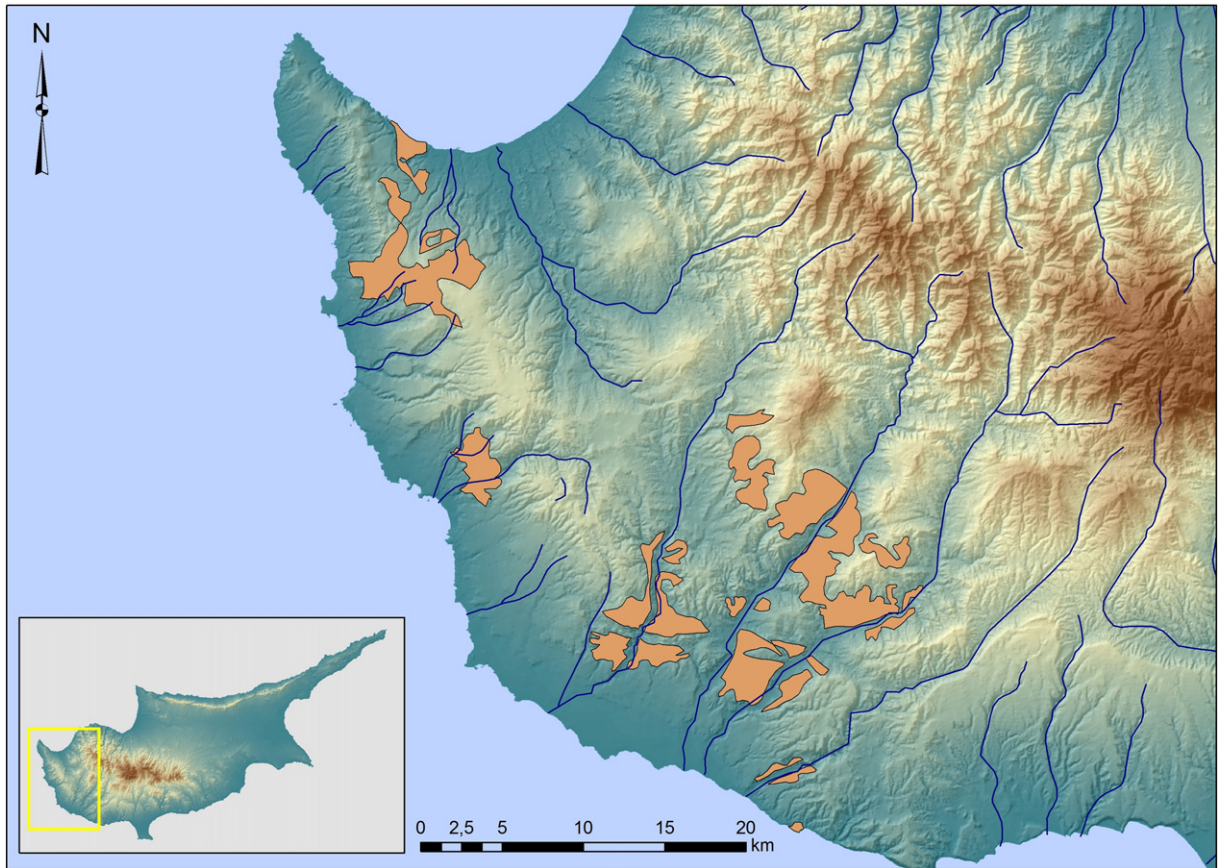| No	Samples mineralogical composition in %												Classes of k-means classifier		
	Calcite	Quartz	Serpentine	Chromite	Dolomite	Clay minerals	Chlorite	Hematite	Feldspar	Pyroxenes	Mica	Talc	K = 3	K = 5	K = 8
1	92	6			1		1						2	4	6
2	23	74				2					1		3	1	3
3	99	1											2	4	4
4	84	4			10				1		1		2	2	8
5	97	3											2	4	4
6	95	4									1		2	4	6
7	94	5			1								2	4	6
8	48	45			1	6							3	5	2
9	96	4											2	4	6
10	97	2			1								2	4	4
11	4	6			3		2	10	75				1	3	1
12	1	92			3			4					3	1	3
13		19	3						71	7			1	3	1
14	89	1			10								2	2	8
15	99	1											2	4	4
16	98	1										1	2	4	4
17	34	66											3	1	2
18	1	99											3	1	3
19	99	1											2	4	4
20		79			1	8		2	3		7		3	1	3
21	99	1											2	4	4
22	8	73			1	7		1	9		1		3	1	3
23	59	9			32								2	5	5
24	39	61											3	1	2
25	94	6											2	4	6
26	80	20											2	2	7
27	57	71				1		1					3	1	2
28	20	72			1	6					1		3	1	3
29	49	42			1	2			4		3		3	5	2
30	98	1			1								2	4	4
31	98	2											2	4	4
32	98	2											2	4	4
33			91	9									1	3	1
34		100											3	1	3
35	95	1											2	4	4

Fig. 5. Map of western Cyprus indicating Mamonia complex, the main resource provenance of mosaic tesserae.

input the known material compositions. The parameter k which preselects the number of clusters has been set to 3, 5, and 8, respectively. The results identify outliers in the samples (e.g. sample 56 with more than 91% of Serpentine) and group "similar" mineralogical composition. In the table, samples represented with the same color for each cluster belong to the same category. As the number of classes' increases, samples with different compositions are divided into subclasses, as expected.

4. Results

4.1. Pre-processing of the spectral signatures

The following experiments were carried out based on the spectral library obtained by collecting all the available spectral signatures, as described in the previous sections. Each spectral signature is associated
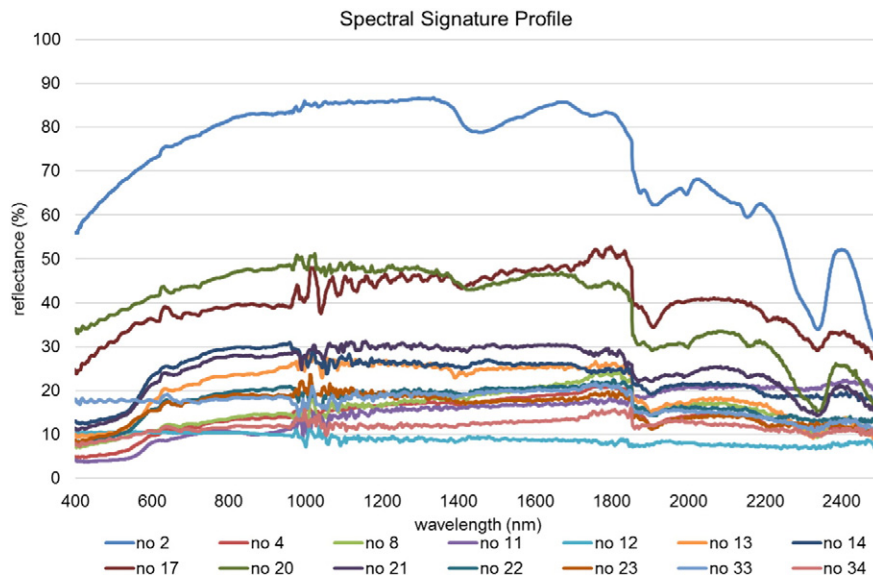

Fig. 6. Example of spectral signature profiles taken from the samples shown in Fig. 4, acquired in the range of 350–2500 nm.

with the description regarding the geological formation and mainly mineralogical characterization of the samples. Based on this information, 43 spectra not presenting a dominant mineralogical element in their composition (above 75%), were removed from the library. The remaining 143 spectra presented a dominant element in their composition, this being either calcite, quartz, or serpentine. This is roughly similar to the categorization of the samples using k-means with k = 3 in Table 1, as two clusters identify materials mostly composed respectively of quartz and calcite, while a third group mostly contains samples composed of other materials.

The spectral library was further analyzed to remove spectral bands with low informational content, which was quantified for this purpose for each spectral band, in order to discriminate bands useful to separate the spectra belonging to the three mineralogical elements listed above.

Initially, the correlation between all the bands was computed to highlight dependency and shared information between each spectral band and all the others. For this purpose, the correlation for any two bands x and y in the spectral library was computed as follows:

$$r_{xy} = \frac{\sum_{i=1}^{n}(x_i - \bar{x})(y_i - \bar{y})}{\sqrt{\sum_{i=1}^{n}(x_i - \bar{x})^2 \sum_{i=1}^{n}(y_i - \bar{y})^2}} \qquad (1)$$

where $\bar{x}$ and $\bar{y}$ are the mean values for any two spectral bands x_i and y_i, computed for n different samples. Fig. 7 displays the correlations for all the bands: high values of correlation indicate high similarity between bands at two given frequencies, while low correlation indicates independence of information. As it is desired to keep all spectral bands which present unique information and have less correlation with others, four main spectral regions were identified, which have high intra-correlation: the visible range from approximately 400 to 700 nm, the Near Infrared (NIR) from 700 to 1400 nm, and two ranges in the Short Wave Infrared (SWIR), approximately from 1450 to 2000 nm and 2000 to 2500 nm respectively. Around 2350 nm a narrow

spectral range appeared to be less correlated to the neighbouring bands, indicating that it could be important to discriminate different targets. The spectral range from 1450 to 2000 nm appeared to be the less informative, as it presents a high correlation with the second portion of the SWIR, but also a relevant correlation with the NIR.

As important as correlation is, this could be however considered insufficient in estimating the discrimination power of a given band or spectral range. For this purpose, measures quantifying the shared information between the data at hand with some kind of existing labelling or categorization must be used.

An important issue of the informational content analysis is the estimation of the amount of information shared by two objects. From Shannon's probabilistic point of view, this estimation is done via the mutual information $I(X, Y)$ between two random variables X and Y, which measures the amount of information that can be obtained about one random variable by observing another, and is defined as:

$$I(X, Y) = \sum_{x,y} p(x, y) \log \frac{p(x, y)}{p(x)p(y)} \qquad (2)$$

where X and Y are two random variables, $p(x)$ is the probability that the variable X generates an outcome with value x, or $p(X = x)$, and $p(x,y)$ is the joint probability of x and y to happen together (Cover and Thomas, 2012). The mutual information is a symmetric quantity $I(X,Y) \geq 0$, with equality if and only if X and Y are independent, i.e. X provides no information about Y. Considering at this stage X as the values assumed by a single spectral band in all samples, and Y as an array in which the dominant materials for each spectrum are labelled from 1 to 3. The mutual information indicates if changes in the values of each band correspond in practice to a change in the dominant object of the spectrum. The computed mutual information between each spectral band and an array containing the dominant material for each acquired sample is reported in Fig. 8.
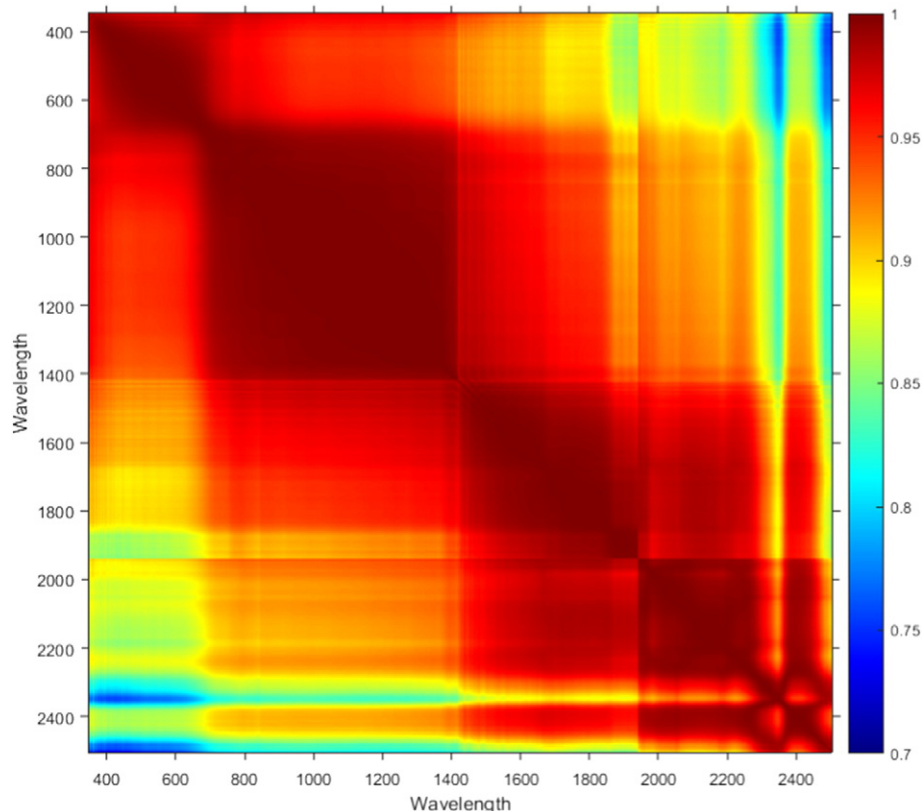

Fig. 7. Correlation between bands for the acquired spectra. Visible, near infrared, and two different ranges in the short wave infrared are easy to identify.
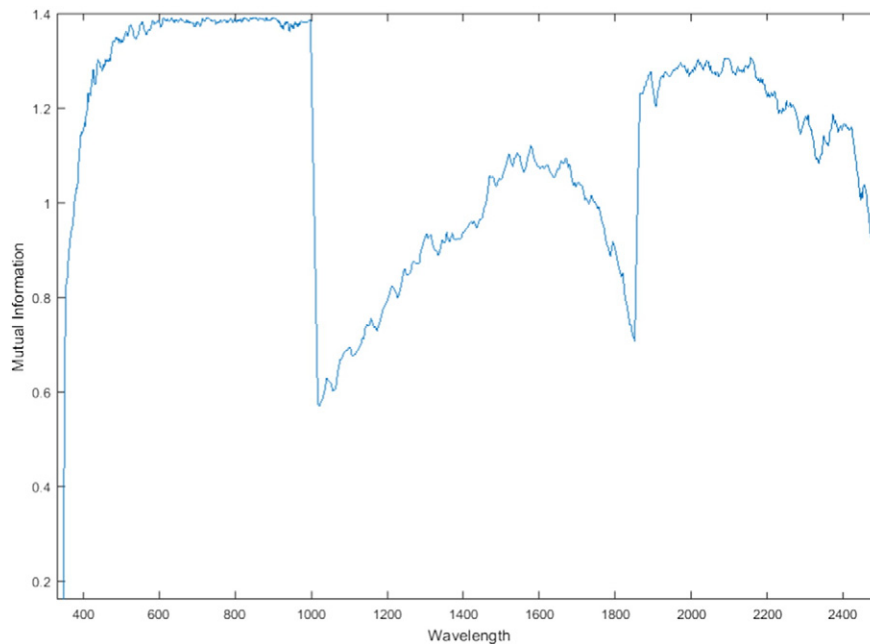
Fig. 8. Mutual Information between each spectral band and the different dominant types of rocks of which the mosaics are composed.

From the mutual information analysis it can beobserved that the spectral range going approximately from 1000 to 1900 nm is not as discriminative as the ranges 400–1000 and 1900–2500, and also relying on previous analysis on correlation it was decided to exclude this range from further analysis, removing the corresponding bands from the dataset, in order to mitigate the effect of Hughes phenomenon, also known as curse of dimensionality, which decreases the accuracy of the results when working in a space with very high dimensionality.

4.2. Spectral unmixing and classification

The process of spectral unmixing aims at decomposing each spectrum into a linear (or less often non-linear) combination of signals. These represent the backscattered solar radiation in each spectral band if the reference spectra are selected within the image. Alternatively, the spectra may be collected in an external spectral library acquired in laboratory. The considered reference signals are typically composed of a single pure material or a homogeneous intimate mixture of materials. Such spectraare often called endmembers (Bioucas-Dias et al., 2012) and must be identified.

For this purpose, Vertex Components Analysis (VCA) (Nascimento and Bioucas Dias, 2005) was applied to the set of spectra in order to identify the purest ones, i.e. spectra which cannot be expressed as a linear combination of the other elements in the dataset. Subsequently, one endmember for each of the three dominant classes described above was identified and a spectral unmixing of all elements in the dataset was carried out.

The output of a spectral unmixing process is a set of abundances values, quantifying the contribution of each reference spectrum to a given pixel. Therefore, a pixel m could be expressed as:

$$m = \sum_{i=1}^{k} x_i s_i + r \tag{3}$$

where $x_1 \dots x_k$ and $s_1 \dots s_k$ are the fractional abundances for the k available and pre-selected reference spectra, while r is a residual vector containing the portion of the signal which cannot be represented in terms of the basis vectors of choice. Therefore, if in a scene only mixtures of two materials in each pixel are presented, for example water and soil, m could be expressed as $m = x_{water} s_{water} + x_{soil} s_{soil} + r$.

The spectral unmixing problem in Eq. (3) was solved by regression using the Least Squares approach, enforcing the non-negativity constraint on the fractional abundances in order not to have negative fractions which would have no physical meaning. Afterwards, a spectrum was assigned to a dominant class according the highest abundancy computed in the spectral unmixing step, i.e. a spectrum was assigned to class 1 if x_1 had the maximum value among the abundances $x_1 \dots x_k$ after solving Eq. (3).

The results of the described classification procedure are reported in Table 2. Here the overall accuracy is the total percentage of samples correctly assigned to their dominant material, while the average accuracy is the mean accuracy obtained per class. Results are encouraging and suggest that different spectra could be successfully categorized at this stage according to the mineralogical composition of the samples. As demonstrated in Table 2, calcite, quartz and serpentine are detected and identified from spectroradiometric analysis with an accuracy of 83.3%, 90% and 100% respectively. The overall accuracy of all samples dominant material is 86%, while the average accuracy per class is 91%. The

Table 2
Classification according to the highest abundance after spectral unmixing results.

		Predicted dominant material					
		Calcite	Quartz	Serpentine	Accuracy	Overall accuracy	Average accuracy
Actual dominant material	Calcite	90	18	0	83.3%	86%	91%
	Quartz	3	27	0	90%		
	Serpentine	0	0	5	100%		

reported confusion matrix highlights some remaining confusion between calcite and quartz. These two minerals have a similar structure and can both assume a variety of colors, such as purple, white, brown, pink and gray (see some examples in Table 1). Therefore, applying spectral unmixing algorithms to mixtures of these two materials is known to present some difficulties (Rodricks, 2007).

5. Discussion

As shown earlier, discriminant analysis of dominant materials used in floor mosaics based on unmixing techniques was achieved with high accuracy. Despite the complexity and the similarity of the samples, the unmixing application was able to detect calcite, quartz and serpentine with an accuracy of 83.3%, 90% and 100% respectively. This high accuracy indicates that such approach can be followed by researchers to rapidly detect and recognize dominant materials in new floor mosaics during field campaigns as well.

The measurements for the above examined geomaterial samples were achieved in an indoor laboratory with controlled environmental conditions. On the contrary, field spectroscopy is susceptible to various types of external noises such as atmospheric effects, shadows etc. Therefore, additional caution should be taken during field spectral signatures recording, while calibrated reference spectralon panel should be also used prior to any measurements. The measurements in the field should be taken between the hours 10:00 a.m. and 14:00 p.m. to minimize the impact of sun illumination from a nadir point of view (Milton et al., 2009; Milton, 1987; Agapiou et al., 2013).

It is important to highlight that the spectral profiles of the samples do not identify directly the dominant minerals, neither automatically retrieve information on the samples chemical composition. However, if a complete spectral library is made available through the systematic collection of measurements, researchers will be able to assign directly a specific spectral profile to a specific mineral and thereafter proceed to its characterization and quantification. For this purpose, it is likely that a large spectral library should be collected: as traditional unmixing algorithms require the number of elements in the library to be smaller than the number of bands in the spectra, sparse unmixing techniques should be employed, which allow approximate solutions of such overdetermined systems (Bioucas-Dias et al., 2012).

Future work on spectroradiometric measurements of floor mosaics includes recording and observing the alterations of spectral profiles, correlated to deterioration factors as a result of environmental impact to the outdoor exposed mosaics.

6. Conclusions

Spectral signatures related to 35 samples of natural rock, directly linked to floor mosaic tesserae identified as such by previous studies, have been acquired in the range of 350–2500 nm and analyzed.The k-means algorithm has been applied using as input features the known rocks compositions in order to have a preliminary categorization of the dataset. Subsequently, the purest spectra have been identified in the dataset to be used to classify the data in groups roughly corresponding to the output of the k-means clustering. Finally, statistical analysis and spectral unmixing techniques have been applied to identify the natural rock-geological provenance of the samples according to their spectral features. The results were found promising since a high accuracy was achieved.

The results of the present paper have been carried out on a small-sized dataset. Future experiments will be validated using a larger number of samples from different geological formations of the island. The final objective is deriving a coherent spectral library to be introduced in the already existing Cypriot floor mosaics database, assisting experts going a step further in identifying relations between mosaic tesserae and their provenance. This database will also be linked to the geographical position of the mineral samples used and the related mosaics, through a Geographical Information System (GIS).

In the future spectroradiometric analysis in situ or in lab could thenoffer a fast preliminarymineralogical characterization of new mosaics/mosaic tesserae, contributing to identify their provenance as well as aid in conservation practices (e.g. selection of materials to integrate missing parts).

Portable spectroradiometers, easy to use in the field, can therefore further assist on-going excavations. Indeed, they can represent a useful toolfor conservation science whenever circumstances require a quick decision (e.g. rescue excavations), eventually in lack of time for the accomplishment of traditional laboratory analysis.The described techniques cannot substitute traditional archaeometric analysis for ancient material identification, but can provide for them an efficient and non-invasive support tool.

References

Agapiou, A., Hadjimitsis, D.G., 2011. Vegetation indices and field spectroradiometric measurements for validation of buried architectural remains: verification under area surveyed with geophysical campaigns. J. Appl. Remote. Sens. 5, 053554. http://dx.doi.org/10.1117/1.3645590.

Agapiou, A., Hadjimitsis, D.G., Sarris, A., Georgopoulos, A., Alexakis, D.D., 2013. Optimum temporal and spectral window for monitoring crop marks over archaeological remains in the Mediterranean region. J. Archaeol. Sci. 40 (3), 1479–1492. http://dx.doi.org/10.1016/j.jas.2012.10.036.

Alexakis, D., Agapiou, A., Hadjimitsis, D.G., Retalis, A., 2012. Optimizing statistical classification accuracy of satellite remotely sensed imagery for supporting fast flood hydrological analysis. Acta Geophys. http://dx.doi.org/10.2478/s11600-012-0025-9.

Bioucas-Dias, J.M., Plaza, A., Dobigeon, N., Parente, M., Du, Q., Gader, P., Chanussot, J., 2012. Hyperspectral unmixing overview: geometrical, statistical, and sparse regression-based approaches. J. Sel. Top. Appl. Earth Obs. Remote Sens. vol. 5 (2), 354–379.

Bonnerot, O., Ceglia, A., Michaelides, D., 2015. "Technology and materials of Early Christian Cypriot wall mosaics". J. Archaeol. Sci. Rep. http://dx.doi.org/10.1016/j.jasrep.2015.10.019 (Available online 18 October 2015), ISSN 2352-409X.

Calia, A., Lettieri, M., Leucci, G., Matera, L., Persico, R., Sileo, M., 2013. The mosaic of the crypt of St. Nicholas in Bari (Italy): integrated GPR and laboratory diagnostic study. J. Archaeol. Sci. 40 (12), 4162–4169.

Charalambous, E., 2011. Geology and the use of mortar in the conservation and manufacture of Cypriot floor mosaics. Proceedings of The 11th Conference of the International Committee for the Conservation of Mosaics (ICCM) [Morocco, Volubilis, 24-27 October 2011] (under publication).

Charalambous, E., 2012. Τεχνολογία κατασκευής των επιδαπέδιων ψηφιδωτών της Κύπρου, Λευκωσία.

Charalambous, N.E., Charalambous, A., Kantiranis, N., Stratis, I., 2009a. Η γεωλογία της Κύπρου και ο ρόλος της στην ανάπτυξη του επιδαπέδιου ψηφιδωτού (δημιουργία βάσης δεδομένων). Report of the Department of Antiquities of Cyprus, Nicosia, pp. 445–548.

Charalambous, N.E., Charalambous, A., Pavlidou, E., Stratis, I., 2009b. Η χρήση του κονιάματος στα υποστρώματα των επιδαπέδιων ψηφιδωτών της Κύπρου. Report of the Department of Antiquities of Cyprus, Nicosia, pp. 549–604.

Cover, T.M., Thomas, J.A., 2012. Elements of Information Theory. John Wiley & Sons.

Department of Geological Survey, 2002. Η Γεωλογία της Κύπρου, Δελτίο Αρ. 10, Υπουργείο Γεωργίας, Φυσικών Πόρων και Περιβάλλοντος, Λευκωσία, Κύπρος.

Hadjicosti, M., Charalambous, E., 2011. Conservation and maintenance of mosaics in Cyprus. Proceedings of The 11th Conference of the International Committee for the Conservation of Mosaics (ICCM) [Morocco, Volubilis, 24–27 October 2011] (under publication).

Michaelides, D., 1987. Cypriot Mosaics. Department of Antiquities, Nicosia, Cyprus.

Milton, E.J., 1987. Principles of field spectroscopy. Remote Sens. Environ. 8 (12), 1807e1827.

Milton, E.J., Schaepman, M.E., Anderson, K., Kneubühler, M., Fox, N., 2009. Progress in field spectroscopy. Remote Sens. Environ. 113, 92e109.

Nascimento, J.M.P., Bioucas Dias, J.M., 2005. Vertex component analysis: a fast algorithm to unmix hyperspectral data. Trans. Geosci. Remote Sens. 898–910.

Piovesan, R., Maritan, L., Neguer, J., 2014. Characterising the unique polychrome sinopia under the Lod Mosaic, Israel: pigments and painting technique. J. Archaeol. Sci. 46, 68–74.

Rodricks, N.K., 2007. Evaluation of spectral unmixing algorithms for mineral identification on mars. ProQuest.